Adsorption and diffusion properties of xylene isomers and ethylbenzene in metal–organic framework MIL-53(Al)

ARTICLE *in* JOURNAL OF POROUS MATERIALS · APRIL 2012

Impact Factor: 1.11 · DOI: 10.1007/s10934-012-9612-z

6 AUTHORS, INCLUDING:

Linhai Duan
Liaoning ShiHua University
40 PUBLICATIONS **254** CITATIONS
SEE PROFILE

Lijuan Song
Liaoning ShiHua University
40 PUBLICATIONS **441** CITATIONS
SEE PROFILE

J Porous Mater (2013) 20:431–440
DOI 10.1007/s10934-012-9612-z

Adsorption and diffusion properties of xylene isomers and ethylbenzene in metal–organic framework MIL-53(Al)

Linhai Duan · Xianying Dong · Yuye Wu · Huailei Li · Li Wang · Lijuan Song

Published online: 5 July 2012

Abstract Adsorption and diffusion behaviour of C8 aromatic isomers, including para-xylene (PX), ortho-xylene (OX), meta-xylene (MX), and ethylbenzene (EB), in metal–organic framework Mil-53(Al) has been systematically investigated by using intelligent gravimetric analyzer, thermogravimetric analysis and molecular simulation respectively. The results indicate that adsorptions of xylene isomers and ethylbenzene molecules in Mil-53(Al) at 303 K present type-I isotherms. The deviation from normal Langmuir model of the isotherms at higher temperature can be, however, found because of the breathing effect of Mil-53(Al) framework. In order to well understand the selective adsorption process of above adsorbates, the diffusion behaviour has been determined and the diffusion coefficient is in the order: OX > PX > MX > EB. The adsorption thermodynamics have been determined by the isotherms at different temperature. A sharp increase of the heat of sorption Q_{st} suggests that a strong interaction between sorbates molecules and between sorbates and the framework appears as the increase of the loading. Two desorption peaks in DTG curves suggests that two sorption locations exist in Mil-53(Al) to C8 alkylaromatics. The molecular simulation results have been used to successfully explain the experimental phenomena and to well understand the underlying adsorption and diffusion features of the systems.

L. Duan · X. Dong · Y. Wu · H. Li · L. Wang · L. Song (✉)
Key Laboratory of Petrochemical Catalytic Science and Technology, Liaoning Shihua University, Fushun 113001, Liaoning, China
e-mail: lsong56@263.net

L. Duan
e-mail: lhduan@126.com

Keywords Adsorption · Diffusivity · Xylene · Metal–organic frameworks

1 Introduction

Metal–organic frameworks (MOFs) consisting with various clusters of metal ions and organic ligands are new kinds of porous material and have received wide attention. This structure has many excellent features such as diversity of composition structure, scalability skeleton, high apparent surface areas, and porosity [1–4]. MOFs have been applied in hydrogen storage [5–8], separation [9–11], heterogeneous catalysis [12, 13], and sensing [14–16]. Adsorption of small molecule such as hydrogen, methane, and carbon dioxide in MOFs has received widely study recently [17–19]. However, the adsorption and diffusion mechanism of larger organic compounds in MOFs is not well understood up to now. Great interest has been paid to adsorption and separation of alkylaromatics in MOFs because MOFs with suitable large pores and the framework consisting of aromatic rings may have potential application for separation of larger organic compounds [20–23].

C8 alkylaromatics, including xylene isomers and ethylbenzene, vastly produced in petroleum processing, play an important role on industrial raw material [24]. But it is very difficult to separate them by using conventional method due to their similar boil points. Therefore, some approaches such as crystallization, barrier separation, and adsorption [25, 26] were applied in solving this problem. Compared with these chemical methods, zeolites and zeolite-like frameworks materials as effective adsorbent have been widely used in selective adsorption process. In the literatures, metal cation-exchanged (Na^+, K^+, and Ba^{2+}) X and Y zeolites present high selectivity of adsorption and

effective separation for the mixtures of xylene isomers [27–30]. In recent years, depending on the pore and framework characteristics of MOFs, selective adsorption and separation for the mixtures of xylene isomers have been reported by many researchers. MIL-47, as pore-filling-dependent selectivity, has been used to separate C8 alkylaromatics [31, 32]. P. M. Marco has studied Zn (BDC)-$(Dabco)_{0.5}$ (BDC 1, 4-benzenedicarboxylate, Dabco 1, 4-diazabicyclo [2.2.2] octane) for the separation of OX from other isomers [22]. Zhi yuan Gu discovered that MOF-5 could elute EB, and MOF-monoclinic showed a preferable adsorption of PX over other isomers [20]. L. Alaerts and V. Finsy found that MIL-53(Al) could separate OX effectively from other C8 alkylaromatics, but the separation efficiency at room temperature is different from that at higher temperature (110 °C) because of the breathing effect of framework of MIL-53(Al) at higher temperature [21, 23, 31].

As the especial structure of MIL-53(Al), adsorption and separation of alkylaromatics mixture reveals enormous potency. Furthermore, the study of alkylaromatics adsorption behaviour in MIL-53(Al) is a guide to obtain higher separation effect for mixture. From the reports by Alaerts [21], changes for the MIL-53 structure during adsorption xylene isomers fore and after were investigated by Rietveld refinements of XRD date sets. Structure analysis concluded that adsorption of OX had a stronger deformation of the channel compared to the effect of adsorption of MX or PX. In the view of this conclusion, L. Alaerts believed that the positions of guest molecules in the MIL-53 structure were the interactions between methyl groups and the framework. Obviously, it is far away to accomplish for the theory research of sorption xylenes and ethylbenzene in MIL-53. In order to implement the better application of MIL-53(Al), it is also necessary to study the mechanism of adsorption and diffusion in this system.

Herein, the adsorption isotherms at different temperature, thermodynamic properties (Q_{st}, ΔG, ΔS and S_a), diffusion coefficient (D/r_0^2) and TG/DTG analysis of xylene isomers and EB in MIL-53(Al) have been systematically investigated using micro gravimetric technique. The location of xylene isomers and EB molecules in the channels of MIL-53(Al) has been determined by molecular simulation method. According to the structure features of MIL-53(Al) and xylene isomers and EB, the differences in adsorption and diffusion behaviour at different temperature and adsorption loading were discussed. Above results shed some light on the improvement of the separation performance for C8 alkylaromatics in MIL-53(Al) effectively and also it is a lead to explore the rarely explored field of the application of larger organic compounds in MOFs.

2 Experimental

2.1 Adsorbent preparation

MIL-53(Al) as was hydrothermally synthesized based on a literature procedure [2], from a mixture of aluminum (III) nitrate $Al(NO_3)_3{\cdot}9H_2O$(AR), terephthalic acid $HO_2C(C_6H_4)CO_2H$ (AR), and H_2O in the molar ratio1: 0.5: 80. After agitating, reactants were introduced in a Teflon-lined stainless steel Parr bomb under autogenous pressure for three days at 220 °C. After filtering off, washing with deionized water, and drying at 100 °C, MIL-53(Al)as or $Al(OH)[O_2C\text{-}C_6H_4\text{-}CO_2]{\cdot}[HO_2C\text{-}C_6H_4\text{-}CO_2H]_{0.70}$ was obtained. Subsequently, in order to purify sample, the unreacted BDC acid in MIL-53(Al) as was removed by heating in air at 330 °C for 72 h, and MIL-53(Al) ht or $Al(OH)[O_2C\text{-}C_6H_4\text{-}CO_2]$ has been obtained. XRD analysis of the sample (Fig. 1) revealed that the framework of MIL-53(Al)ht was successfully formed and the excess terephthalic acid in the pores was removed. Surface area, pore size and pore volume are measured respectively, according to the BET (Barrett-Emmett-Tellter) model by nitrogen adsorption and desorption experiment at 77 K (Fig. 2) used IGA-002/003 intelligent weight analyzer (see Sect. 2.2). After removal of guest molecules, surface area, pore size and pore volume reach 1,487 m^2/g, 0.85 nm and 0.53 cm^3/g respectively.

2.2 Isotherms and temperature programmed desorption (TPD)

Intelligent gravimetric analyzer (IGA) (Hiden Analytical Ltd., Warrington, UK) was employed in this study. This apparatus can not only measure the adsorption–desorption

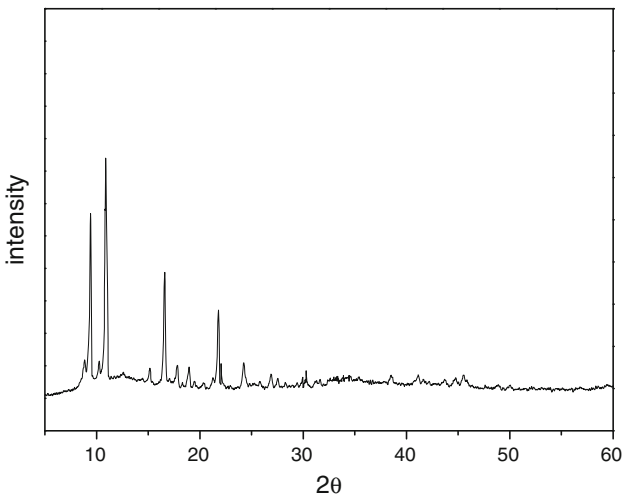

Fig. 1 XRD of MIL-53(Al) after calcinations at 603 K in air

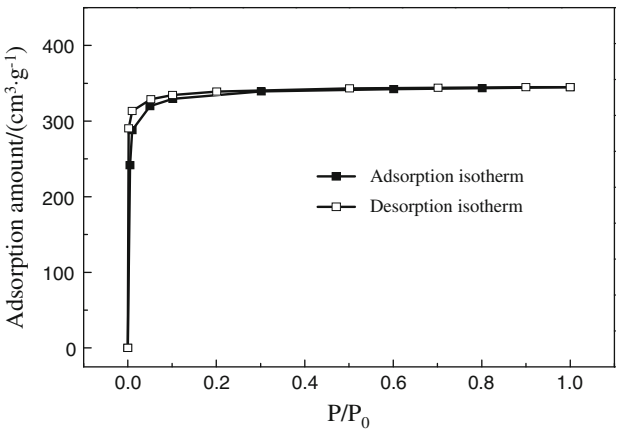

Fig. 2 N_2 adsorption and desorption isotherms on MIL-53(Al) at 77 K

isotherms but also determine the corresponding kinetics of adsorption and desorption at each pressure step. As the system utilizes a sensitive microbalance (resolution of 0.1 μg) automatical by computer controlling to measure the weight of the sample sorbents and employs an accurate pressure control system (resolution: 1/16,000 of range) to regulate pressure set-point and ramp control, it is guaranteed to higher accuracies and stabilities. Herein, the adsorption isotherms of xylenes were determined by loading 100 mg samples and then outgassing under a vacuum of $<10^{-3}$ Pa at 603 K for about 20 h. The temperature was then decreased to the measurement temperature and maintained by either a water bath or a furnace. The sorbates were introduced into the system and the sorption isotherms were obtained with equilibrium pressures step by step.

The curve of temperature programmed desorption (TPD) was also obtained by IGA. After the adsorption achieved equilibrium, the sample was gradually heated from room temperature to objective temperature at a rate of 5 °C/min along with the nitrogen as carrier gas. The weight lose of sorbent can be automatically recorded versus temperature, so the thermogravimetric (TG) curve was obtained, and differential thermogravimetry (DTG) was also easily got.

2.3 Molecule simulation

The adsorption configurations for C8 alkylaromatics adsorbed in MIL-53(Al) were calculated using Grand canonical Monte Carlo (GCMC) method with sorption program in Material Studio 5.5 package of Accelrys Ltd. The framework of MIL-53(Al) was constructed from experimental powder X-ray diffraction (PXRD) data [2]. The Van der Waals interaction was treated with a 12-6 Lennard–Jones (LJ) potential. The COMPASS force filed was used to describe the interactions between framework and adsorbates. The cutoff distance for the calculation of the van der Waals potential energy was taken as 12.0 Å, while the electrostatic contributions was estimated using the Ewald summation. The simulation box consisted of 8 ($2 \times 2 \times 2$) unit cells was used as rigid with frozen atoms during simulation. Periodic boundary conditions were applied in all simulations. A total of 3,000,000 equilibration cycles and 3,000,000 production cycles were used for each simulation.

3 Results and discussion

3.1 Adsorption equilibrium

Adsorption isotherms of OX, MX, PX, and EB in MIL-53(Al) at 303, 333 and 373 K are shown in Fig. 3. For 303 K, one can see that the isotherms of OX, MX and PX, which are fitted with the classical Langmuir equation, rise steeply and quickly reach a plateau. But the isotherm of EB has not achieved a plateau in the test concentration range. Meanwhile, the corresponding diffusion coefficient of EB is lower than other adsorbates, which would be discussed in Sect. 3.3, meaning that the diffusion behaviour for EB in Mil-53(Al) play an important role on the adsorption process. Moreover, the saturation capacities of OX and PX in Mil-53(Al) reach at 3.4 molecules per unit cell (m/uc) and 3.3 m/uc, respectively, which are larger than MX and EB.

With the increasing adsorption temperature, the breathing effect has been found in the adsorption isotherms of sorbates in Mil-53(Al), so adsorption isotherms have two steps at 333 and 373 K, respectively. At 333 K, the isotherms of PX, OX and MX appear slight step, indicating that the breathing effect of the framework begins to occur. When the sorption temperature rises to 373 K, it is obvious that there are two adsorption steps for isotherms.

For 373 K, the capacity of OX jumps steeply from 0.6 to 2.7 m/uc at a partial pressure of 3 mbar, however, others are relative gentleness. MX shows a slow increase from 0.7 to 1.9 m/uc after a flat from 1 to 4 mbar. With a longer flat, PX starts the second step at 6 mbar, and tends to equilibrium at 12 mbar, corresponding to 2.4 m/uc. Interestingly, EB shows a slight kink at about 0.5 mbar, and then increases steeply until almost equilibrium. EB shows the smallest capacity among all of these sorbates, which only has adsorption capacity of 1.2 m/uc.

3.2 Thermodynamics

The interaction of sorbate-sorbent system at the pressure tending to zero was characterized by Henry constants (K′). Figure 4 shows the virial plots of ln (p/q) versus q, where p

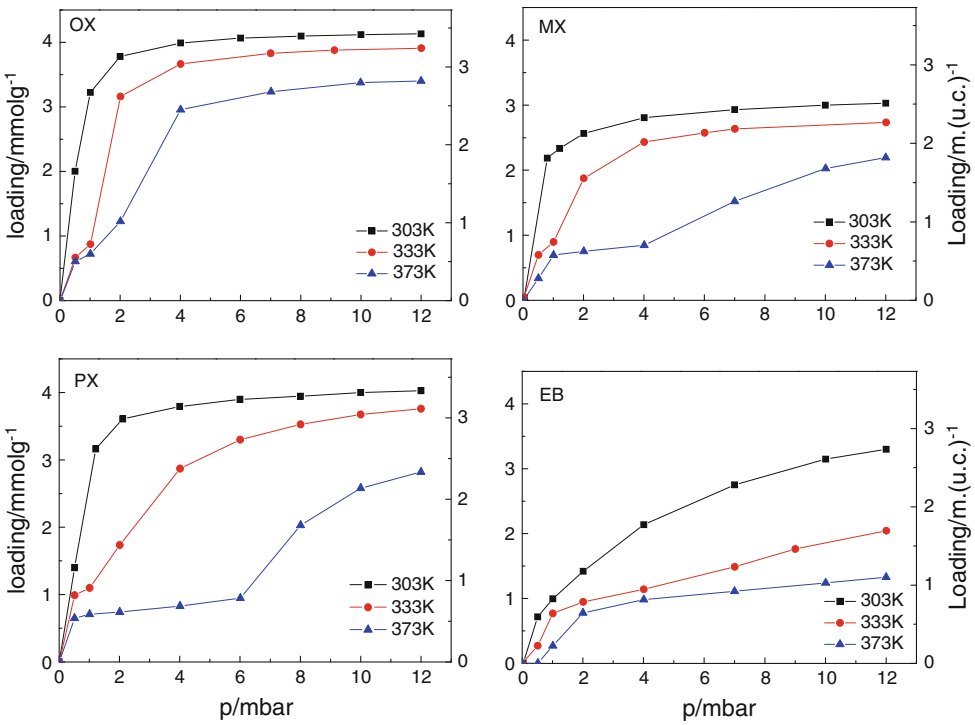

Fig. 3 Adsorption isotherms of ortho-xylene (*OX*), meta-xylene (*MX*), para-xylene (*PX*) and ethylbenzene (*EB*) in MIL-53(Al) at 303, 333 and 373 K

is the partial pressure (Pa) and q the loading (mol/kg). These plots have linear relationships in the low coverage; therefore, Henry constants can be obtained from the extrapolation of the virial isotherms to zero coverage. Adsorption enthalpy at zero coverage (ΔH_0) was investigated from the temperature dependence of the Henry constants (K′) using the van't Hoff equation:

$$K' = K_0 e^{\Delta H_0/RT} \quad (1)$$

where K_0 is the pre-exponential factor of the Henry's constant, R is the ideal gas constant, and T is the temperature.

The van't Hoff plots of lnK′ versus 1/T reveal the adsorption enthalpy at zero coverage, and from the Fig. 5, zero coverage adsorption enthalpy (ΔH_0) can be easily obtained, which are tabulated in Table 1. From the table,EB and OX has large adsorption enthalpy value, and that of PX is the smallest. It displays that both OX and EB have stronger interaction with the framework at the beginning of adsorption.

The dependence of the isosteric heats of sorption on the sorbate loading for alkyl aromatics has been shown in Fig. 6. From the Fig. 6, the heats of sorption for sorbates have varying degrees of enhancement at loading from 0.5 to 1.5 m/uc. When the adsorption amounts are more than 1.5 m/uc, the isosteric heats of sorption for the adsorbates reduce slowly. The heats of sorption for sorbates varied significantly with loading can be verified the breathing effect for MIL-53(Al) framework at low pressure.

As the lower sorption coverage, molecules with a single-file arrangement orientate along the long axis of the rhombic-shaped lattice and interaction occurs between alkyl chains of sorbates and the framework, even the framework had contraction as presented in Fig. 7a. At loading of 0.5 m/uc, the heat of sorption for OX is maximum, which means that interaction between methyl of OX molecules and the framework is the strongest. Accordingly, interaction between PX molecules and framework is the weakest. This phenomenon may be explained by the change of the framework of MIL-53. Finsy [23] reported that adsorption of small amount number alkyl aromatic molecules caused framework contraction and this contracted pore structure would be reopened with the increase loading. Under the framework contraction, OX has a stronger effect with the framework lattice and PX is the weakest. Above result is also very corresponding with the report from Alaerts [21], who analyzed the changes of the MIL-53 structure before and after adsorption of xylene isomers by Rietveld refinements of XRD date sets.

At loading from 0.5 to 1.5 m/uc, the sorption heats of PX and MX increased by 19 and 16 kJ/mol, respectively, which are larger than that of OX and EB. The increase of sorption heats indicates that another kind of interaction appears with growing of the sorption coverage. This may be induced by reopened of the framework with the increase loading and π–π effect between the aromatic sorbate molecules and between sorbates and terephthalate ligands of the framework, as presented in Fig. 7b, c. The π–π effect

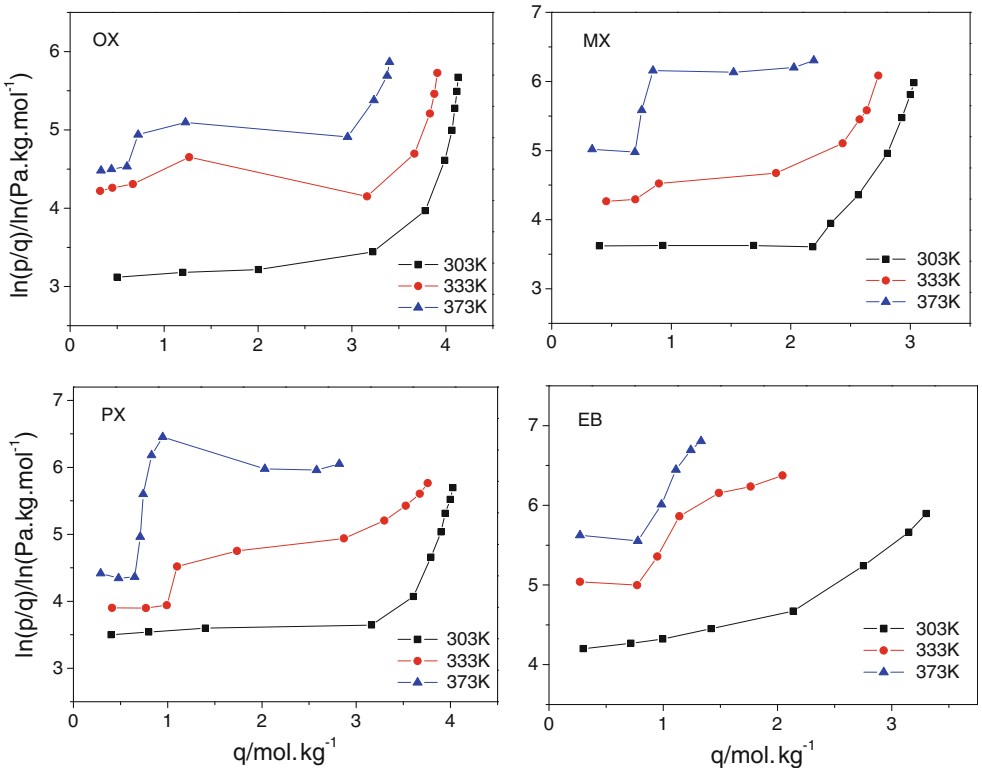

Fig. 4 Ln (p/q) versus q for the analysis of the virial isotherm of ortho-xylene (*OX*), meta-xylene (*MX*), para-xylene (*PX*) and ethylbenzene (*EB*) on MIL-53(Al)

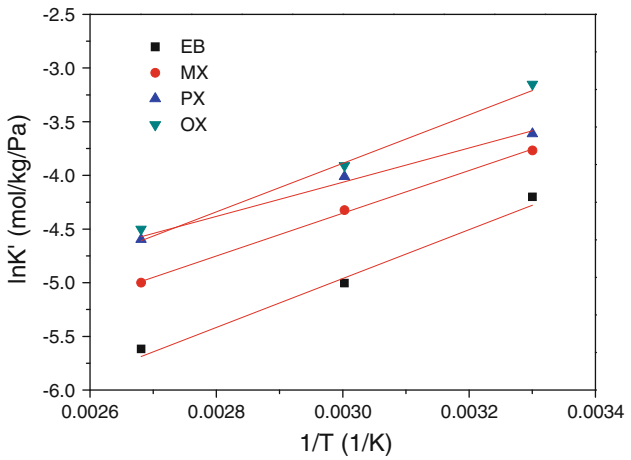

Fig. 5 Van't Hoff plots of ethylbenzene (*EB*), meta-xylene (*MX*), para-xylene (*PX*) and ortho-xylene (*OX*) on MIL-53(Al)

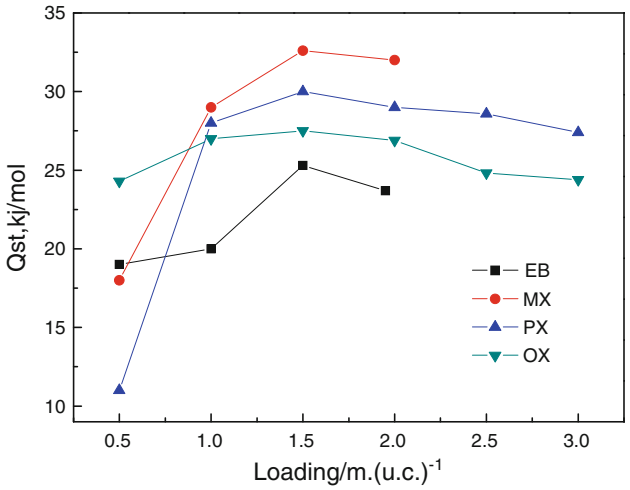

Fig. 6 Dependence of the isosteric heat of sorption (*Qst*) of ethylbenzene (*EB*), meta-xylene (*MX*), para-xylene (*PX*) and ortho-xylene (*OX*) in MIL-53(Al) on the sorption coverage

Table 1 Adsorption enthalpy at zero coverage (ΔH_0) of all C8 alkyl aromatic components

	OX	PX	MX	EB
$-\Delta H_0$ (kJ/mol)	18.7	13.2	16.5	18.9

for PX is the strongest and that for EB is weaker due to steric hindrance of its alkyl. The desorption temperature of PX at 300 °C is the highest in curve of DTG, can testify the strongest π–π effect for PX. The changes of ΔG, ΔS and S_a can also support this conclusion in Figs. 8, 9, and 10.

3.3 Kinetics

At 303 K, the comparison for diffusion rates of EB, MX, PX, and OX in MIL-53(Al) is obviously shown in Fig. 11.

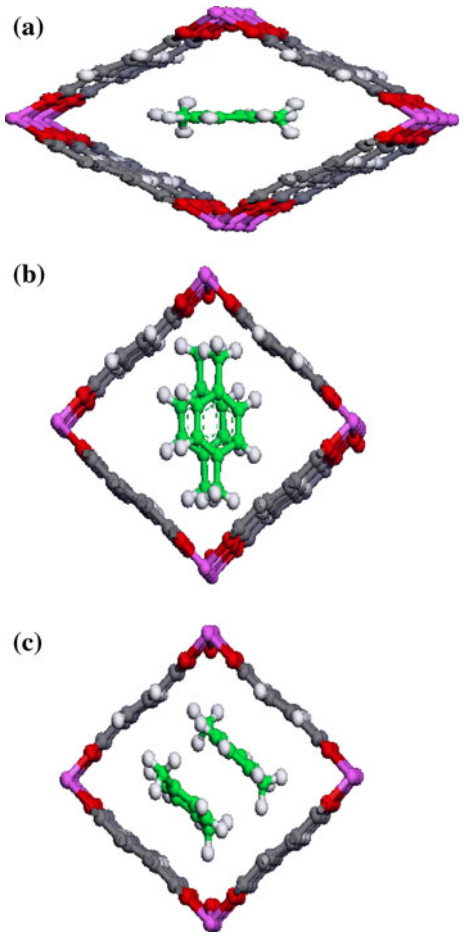

Fig. 7 Patterns of sorbed PX molecules in **a** contracted MIL-53(Al) and **b**, **c** reopened MIL-53 (Al) ht

We can see that the relationship for diffusion rates is OX > PX > MX > EB, which is corresponding with the adsorptive capacities in adsorption isotherms of those adsorbates at this temperature in Fig. 3. Sorbate molecules orientate along the long axis of the rhombic-shaped lattice paralleling to the channel direction. Short molecular length of OX may explain the phenomenon of large diffusion rate of OX. As longer alkyl chain, EB appears slow diffusion because ethyl group makes steric hindrance, which could explain the lower adsorption amount and difficulty to achieve equilibrium in the adsorption isotherm.

At 373 K, diffusion coefficient of EB, MX, PX, and OX in MIL-53(Al) versus loading is shown in Fig. 12. From adsorption isotherm of OX at 373 K in Fig. 3, the fastest-growing stage of adsorption capacity is shown at the loading of 1.0 to 2.5 m/uc, in which range the rate of diffusion also appears increment. However, at loading of about 2.7 m/uc, OX has a maximum diffusion rate comparing with other loadings. Therefore, the diffusion appears lag in phase. Similarly, other adsorbates also turn up this phenomenon. These suggest that, with opening of the framework at 373 K, the pores of MIL-53(Al) assembled with amount of sorbates rapidly, and then diffusion arises to high speed leading to a larger adsorption capacity.

3.4 Thermal analysis

The thermal analytical thermograms of desorption C8 alkylaromatics samples from MIL-53(Al) are shown in Fig. 13. We found two overlapped peaks, versus T_{max} at 235 and 280 °C respectively, in the DTG curve of OX, indicating that there are two adsorption features between the sorbate molecules and the framework of MIL-53(Al). The peak versus higher temperature in the DTG curves suggests that a stronger reaction, which can be ascribed to the π–π interaction by benzene rings of OX with terephthalate ligands of the MIL-53(Al). However, the lower temperature peak presents weaker interaction, which is induced by the methyl groups of adsorbate interacting with the carboxylate groups of MIL-53(Al). While the TG curve of MX shows two-step desorption process and the DTG curve has two conterminal peaks with T_{max} at 210 and 260 °C, respectively. This means that MX molecules interact with the framework of MIL-53(Al) also by means of two adsorption interactions, which are similar with that of OX molecules. The TG curve of PX shows notable steps, and DTG curve has three peaks with T_{max} at 130, 200 and 300 °C, respectively. The latter two peaks are similar with that of OX and MX, which indicate two different adsorption interactions between adsorbates and framework of MIL-53(Al). However, the weaker intensity peak at 130 °C, which close to the boiling point of PX (138 °C), indicates that original sorption equilibrium may be destroyed, and faint physical desorption occurs. Moreover, from the DTG analysis for EB, we find that the first peak is the widest with T_{max} in the range of 170–215 °C, which may be arose from the complicated interactions between the longer ethyl chain of EB molecule with the framework of MIL-53(Al). The second peak of EB in DTG curve with T_{max} at 280 °C also presents the π–π interactions between benzene rings of EB and terephthalate ligands.

By contrasting the desorption temperature in DTG curves, it can be found that the adsorption interactions between alkyl radical and framework in MIL-53(Al) are in the order of OX (235 °C) > MX (210 °C) > PX (200 °C) > EB (170 °C to 215 °C). This result indicates that interaction between methyl groups of OX and framework is slight stronger than that of the other three adsorbates. T_{max} of PX at 300 °C is higher than that of others, demonstrating that the π–π interaction between PX molecules and the framework is the strongest.

3.5 Location analysis from molecular simulation

In order to further certify above experiment results, molecular simulation method has been used to study the adsorption orientation of sorbates in MIL-53(Al), and the

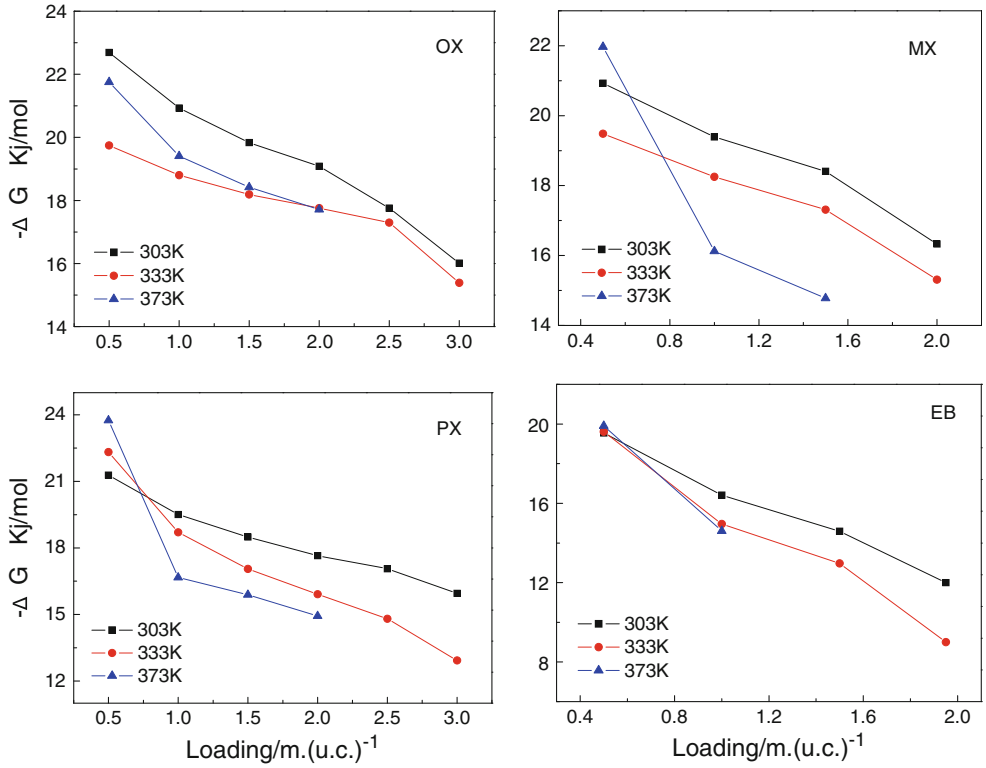

Fig. 8 Dependence of the free energy change of sorption (ΔG) of ortho-xylene (*OX*), meta-xylene (*MX*), para-xylene (*PX*) and ethylbenzene (*EB*) in MIL-53(Al) on the sorption coverage

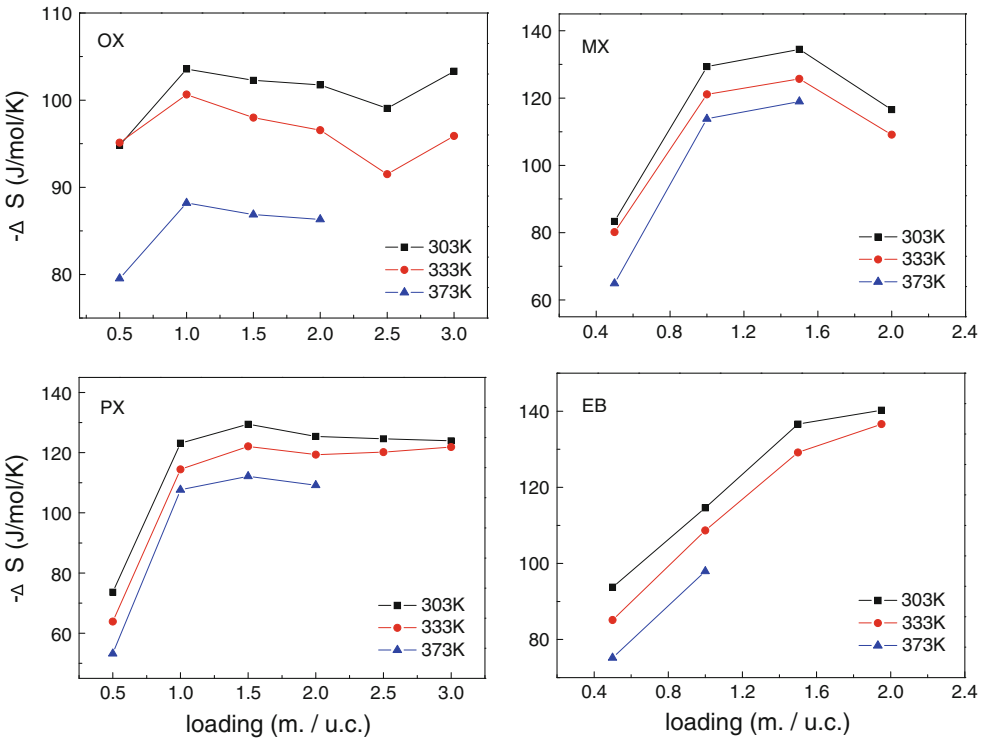

Fig. 9 Dependence of the entropy change of sorption (ΔS) of ortho-xylene (*OX*), meta-xylene (*MX*), para-xylene (*PX*) and ethylbenzene (*EB*) in MIL-53(Al) on the sorption coverage

results are shown in Fig. 14. According to the adsorption configuration in Fig. 14, two kinds of adsorption orientation can be obtained, i.e., sorbates paralleling with the terephthalate ligands of the framework and presenting transverse in lattices, which are well agreed with two desorption peaks in DTG analysis in Fig. 13.

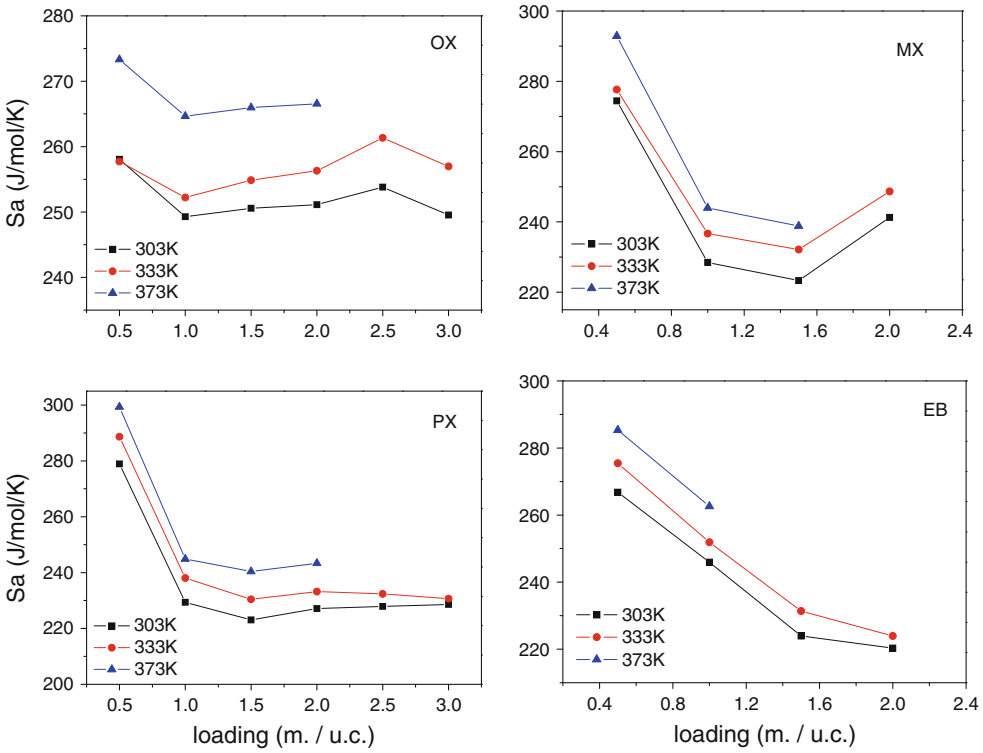

Fig. 10 Dependence of the entropy of sorption (*Sa*) of ortho-xylene (*OX*), meta-xylene (*MX*), para-xylene (*PX*) and ethylbenzene (*EB*) in MIL-53(Al) on the sorption coverage

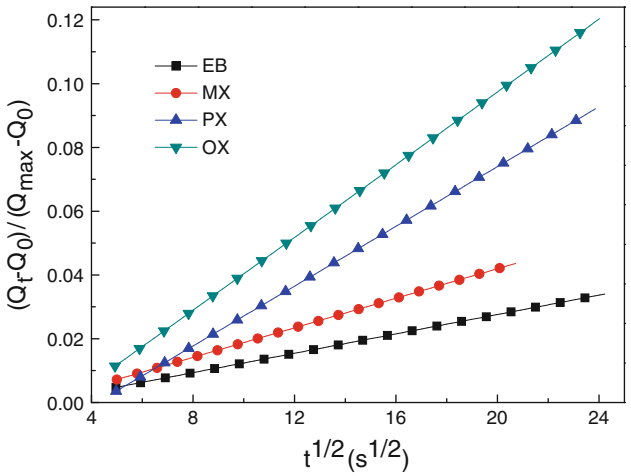

Fig. 11 Uptake of ethylbenzene (*EB*), meta-xylene (*MX*), para-xylene (*PX*) and ortho-xylene (*OX*) in MIL-53(Al) showing the conformity with the Fick's equation for short time at 303 K at the beginning of the sorption

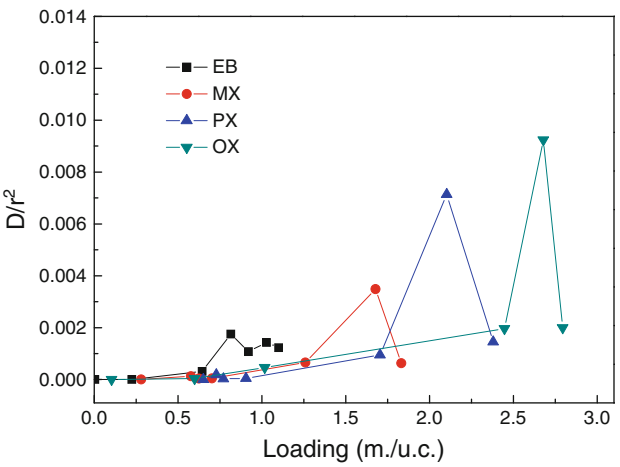

Fig. 12 Diffusion coefficient of ethylbenzene (*EB*), meta-xylene (*MX*), para-xylene (*PX*) and ortho-xylene (*OX*) in MIL-53(Al) at 373 K as a function of loading

The parallel mode of sorption configuration is generated by π–π interactions between benzene rings of sorbates molecules and terephthalate ligands of MIL-53(Al). For PX, the molecules appear perfect parallel with the terephthalate ligands, which leads to strong π–π interactions between PX molecules and framework. By analyzing adsorption configuration of OX, MX and EB in the pore of MIL-53(Al) framework, it can be noted that these parallel shows a tilt caused by leaning one side of the alkyl radicals. Therefore, the intensity of this kind of π–π interaction for OX, MX and EB molecules is weaker than that for PX molecules. These results are also well consistence with the DTG results in Fig. 13, demonstrating that the T_{max} of PX is higher than that of OX, MX and EB. Furthermore, in this adsorption configuration, the π–π interactions can also occurs between the sorbates molecules.

Moreover, it can be found that another sorption position is very obvious in Fig. 14, i.e., the methyl group of sorbates interact with the framework and without the parallel

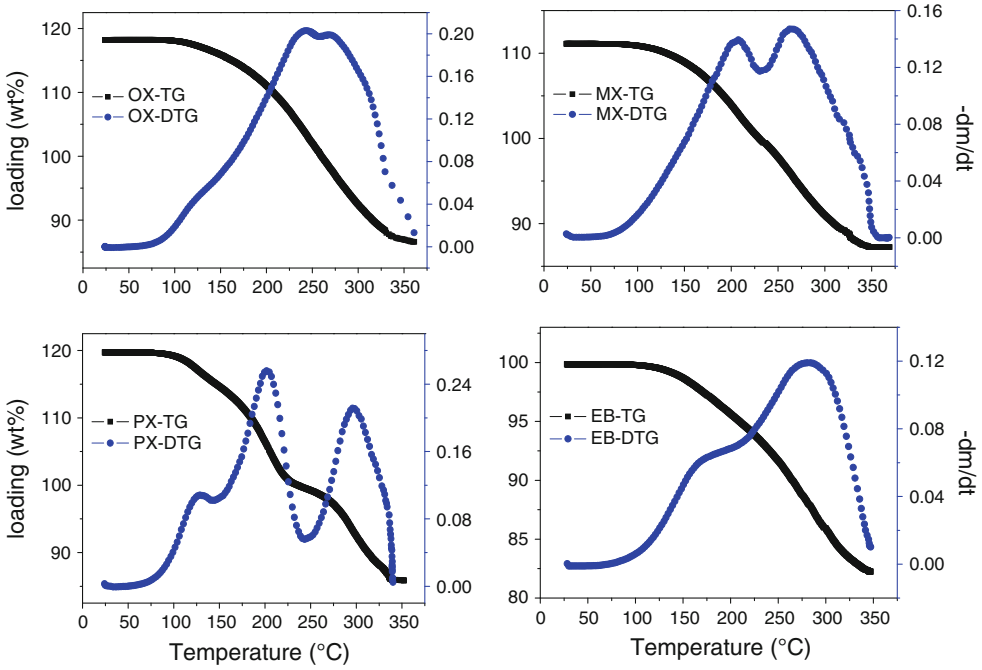

Fig. 13 TG and DTG profiles of ortho-xylene (*OX*), meta-xylene (*MX*), para-xylene (*PX*) and ethylbenzene (*EB*) in MIL-53(Al)

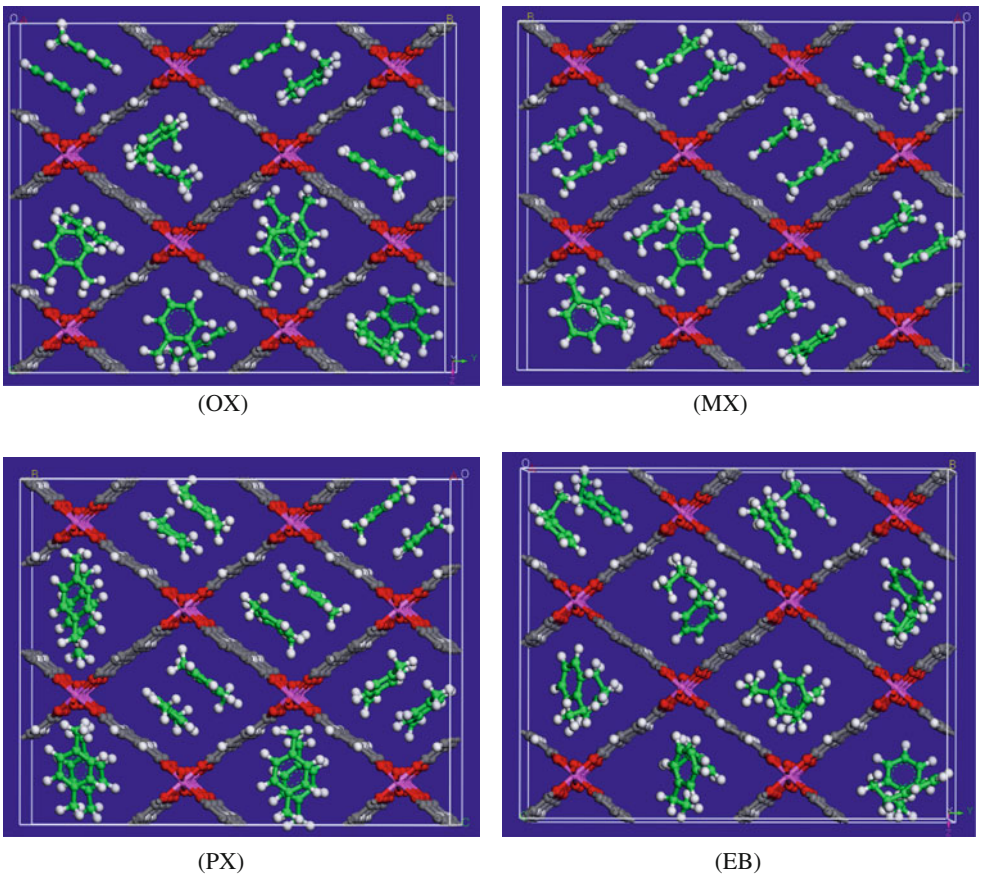

Fig. 14 Sorption location of ortho-xylene (*OX*), meta-xylene (*MX*), para-xylene (*PX*) and ethylbenzene (*EB*) in MIL-53(Al) investigated by molecular simulation in 100 kPa at 303 K

orientation between sorbates and the framework. For OX molecules, the second sorption position is that both methyl groups interact with carboxylate groups of the host. But to MX, one methyl group interacts with carboxylate groups, at the meantime, another methyl group and C2 carbon atom of the aromatic ring of MX effect with an aromatic ring of

the framework. PX molecules can interact with the carboxylate groups via only one metal group. Ethyl groups not only can effect with carboxylate groups in angle of the lattice, but also may parallel with terephthalate ligands. Above complicated effects can well explain the wide desorption peak shown in DTG curve of EB in Fig. 13.

4 Conclusions

The results of this study show that the C8 isomeric aromatic hydrocarbons have different adsorption and diffusion behaviour in MIL-53(Al). The sorption isotherms of xylene and EB in MIL-53 at 303 K can be well fitted by the Langmuir model, while at 333 and 373 K, a dual-site Langmuir (double Langmuir) model has to be used to fit the isotherms of these systems. This deviation of the isotherms from normal Langmuir model can be ascribed to the framework opening as breathing effect.

The diffusion rates at low loading is in the order OX > PX > MX > EB, which is corresponding with the adsorptive capacities in adsorption isotherms. The higher diffusion rate of OX is due to the short molecular length of OX, while the lower diffusion rate for EB is because of the longer alkyl chain EB molecules.

The thermodynamic characteristics of xylenes and EB in MIL-53 suggest that sorbate-sorbent interactions and the sorbate–sorbate interactions vary with adsorption coverage. At the low adsorption coverage, the interaction is mainly between methyl groups and carboxylate groups of the framework. With increasing of the loading, π–π effect between sorbate molecules and between sorbates and the framework is increased. The TG/DTG curves have certified that these two locations exist during the sorption process of xylene and EB in MIL-53. Among the interactions mainly generated by alkyl radicals with the framework, the OX is the strongest compared with PX, MX, EB. While considering π–π interaction, the PX is larger comparing to other sorbates. Furthermore, molecular simulation have been found to be very useful in helping to demonstrate, at a molecular level, the underlying features controlling the adsorption and diffusion of these sorbates in MIL-53(Al).

Acknowledgments Authors are grateful for the financial support provided for this research by the National Nature Science Foundation of China (No. 21076100).

References

1. J.L.C. Rowsell, O.M. Yaghi, Microporous Mesoporous Mater. **73**, 3 (2004)
2. T. Loiseau, C. Serre, C. Huguenard, G. Fink, F. Taulelle, M. Henry, T. Bataille, G. Férey, Chem. Eur. J. **10**, 1373 (2004)
3. G. Férey, C. Mellot Draznieks, C. Serre, F. Millange, J. Dutour, S. Surblé, I. Margiolaki, Science **309**, 2040 (2005)
4. O.M. Yaghi, M.O. Keeffe, N.W. Ockwig, H.K. Chae, M. Eddaoudi, J. Kim, Nature **423**, 705 (2003)
5. J.G. Vitillo, L. Regli, S. Chavan, G. Ricchiardi, G. Spoto, P.D.C. Dietzel, S. Bordiga, A. Zecchina, J. Am. Chem. Soc. **130**, 8386 (2008)
6. Y. Kubota, M. Takata, R. Matsuda, R. Kitaura, S. Kitagawa, T.C. Kobayashi, Angew. Chem. **118**, 5054 (2006)
7. P.L. Llewellyn, S. Bourrelly, C. Serre, Y. Filinchuk, G. Férey, Angew. Chem. **118**, 7915 (2006)
8. V. Finsy, L. Ma, L. Alaerts, D.E. De Vos, G.V. Baron, J.F.M. Denayer, Microporous Mesoporous Mater. **120**, 221 (2009)
9. J.W. Yoon, S.H. Jhung, Y.K. Hwang, S.M. Humphrey, P.T. Wood, J.S. Chang, Adv. Mater. **19**, 1830 (2007)
10. M.H. Alkordi, Y. Liu, R.W. Larsen, J.F. Eubank, M. Eddaoudi, J. Am. Chem. Soc. **130**, 12639 (2008)
11. Q.M. Wang, D. Shen, M.L. Lau, S. Deng, F.R. Fitch, N.O. Lemcoff, J. Semanscin, Microporous Mesoporous Mater. **55**, 217 (2002)
12. C.D. Wu, W.B. Lin, Angew. Chem. Int. Ed. **46**, 1075 (2007)
13. C. Serre, F. Millange, C. Thouvenot, M. Nogues, G. Marsolier, D. Louer, J. Am. Chem. Soc. **124**, 13519 (2002)
14. S.Q. Ma, D.F. Sun, X.S. Wang, H.C. Zhou, Angew. Chem. Int. Ed. **46**, 2458 (2007)
15. B. Chen, L. Wang, F. Zapata, G. Qian, E.B. Lobkovsky, J. Am. Chem. Soc **130**, 6718 (2008)
16. T.K. Maji, R. Matsuda, S. Kitagawa, Nat. Mater. **6**, 142 (2007)
17. F. Hiroyasu, O.M. Yaghi, J. Am. Chem. Soc. **131**, 8875 (2009)
18. B. Kesanli, W.B. Lin, Coord. Chem. Rev. **246**, 305 (2003)
19. B. Panella, M. Hirscher, H. PItter, U. MIller, Adv. Funct. Mater. **16**, 520 (2006)
20. Z.Y. Gu, D.Q. Jiang, H.F. Wang, X.Y. Cui, X.P. Yan, J. Phys. Chem. **114**, 311 (2010)
21. L. Alaerts, M. Maes, L. Giebeler, P.A. Jacobs, J.A. Martens, D.E. De Vos, J. Am. Chem. Soc. **130**, 14170 (2008)
22. M.P.M. Nicolau, P.S. Bárcia, J.M. Gallegos, B.L. Chen, J. Phys. Chem. **113**, 13173 (2009)
23. V. Finsy, C.E.A. Kirschhock, G. Vedts, M. Maes, L. Alaerts, D.E. De Vos, J.F.M. Denayer, Chem. Eur. J. **15**, 7724 (2009)
24. M. Minceva, A.E. Rodrigues, AIChE J. **53**, 138 (2007)
25. K. Iwayama, M. Suzuki, Stud. Surf. Sci. Catal. **83**, 243 (1994)
26. Z.P. Lai, T. Michael, Ind. Eng. Chem. Res. **43**, 3000 (2004)
27. R. Hulme, R. Rosensweig, D. Ruthven, Ind. Eng. Chem. Res. **30**, 752 (1991)
28. D.M. Ruthven, M. Goddard, Zeolites **6**, 275 (1986)
29. C. Perego, P. Ingallina, Catal. Today **73**, 3 (2002)
30. V. Cottier, J.P. Bellat, M.H. Simonot Grange, J. Phys. Chem. **101**, 4798 (1997)
31. L. Alaerts, C.E.A. Kirschhock, M. Maes, D.E. De Vos, Angew. Chem. Int. Ed. **46**, 4293 (2007)
32. V. Finsy, H. Verelst, L. Alaerts, D. De Vos, G.V. Baron, J.F.M. Denayer, J. Am. Chem. Soc. **130**, 7110 (2008)